

# Unexpected large thermal rectification in asymmetric grain boundary of graphene

Hai-Yuan Cao<sup>a</sup>, Hongjun Xiang<sup>a</sup>, Xin-Gao Gong<sup>a</sup>

<sup>a</sup>*Key Laboratory of Computational Physical Sciences (Ministry of Education), State Key Laboratory of Surface Physics, and Department of Physics, Fudan University, Shanghai 200433, P.R. China*

---

## Abstract

We have investigated the lattice thermal transport across the asymmetric tilt grain boundary between armchair and zigzag graphene by nonequilibrium molecular dynamics (NEMD). We have observed significant temperature drop and ultra-low temperature-dependent thermal boundary resistance. More importantly, we find an unexpected thermal rectification phenomenon. The thermal conductivity and Kapitza conductance is direction-dependent. The effect of thermal rectification could be amplified by increasing the difference of temperature imposed on two sides. Our results propose a promising kind of thermal rectifier and phonon diodes based on polycrystalline graphene without delicate manipulation of the atomic structure.

*Keywords:* A. Graphene, C. Grain boundary, D. Kapitza conductance, D. Thermal rectification

*PACS:* 61.48.Gh, 61.72.Lk, 61.72.Mm, 66.70.-f, 73.40.Ei

---

Graphene, a two dimensional honeycomb lattice, is well recognized as one of the most promising materials in future electronics and nanotechnology[1, 2]. Numerous previous studies have shown that the monolayer graphene samples with perfect lattice structure exhibit outstanding electronic, thermal, mechanical and optical properties[3, 4, 5, 6]. While the size of graphene flakes from mechanical exfoliated is too small to be utilized for mass production of functional devices, chemical vapor deposition (CVD) enables the synthesis of large-area, high-quality and low-cost graphene sheets[7, 8, 9]. Due to the imperfections of metal foils in the growth process, the grains inevitably nucleate during the growth which results to the formation of grain boundaries in graphene sheets[10, 11]. Understanding the effect of the grain boundaries on the mechanical, electronic, and thermal properties is very helpful and necessary for future applications of the larger-scale polycrystalline graphene.

Recently, several studies have shown that the grain boundaries have cru-

---

*Email address:* xggong@fudan.edu.cn (Xin-Gao Gong)

cial influence on the mechanical and electronic properties. For the mechanical property, the grain boundaries with high density of topological defects show anomalous characteristics of mechanical strength[12]. In the case of charge transportation, the charge mobility depends on the grain size which is determined by the grain boundaries[9]. Furthermore, the transmission of the charge carrier across the grain boundary depends on the symmetry of the atomic structure. The charge transport of the symmetric grain boundary reveals high transparency while that of the asymmetric grain boundary emerges almost perfect reflection[13]. Experiments have shown that the line defects like grain boundary can be one of the most powerful ways to manipulate electronic properties at nanoscale[14, 15, 16]. For the thermal transport, although there have been many studies on the point defects including vacancies[17], Stone-Wales defects[18] and isotope defects[19], the effect of line defects like grain boundary on thermal conductivity is still far from well-understood. In a recent work [20], thermal transport across the tilt grain boundaries with simplest symmetric atomic structure has been considered. Sudden temperature drop at the grain boundary and superior boundary conductance has been observed in that system[20]. There is still a long way for us to further explore and understand the impact of one-dimensional global defects on the thermal transport of graphene. Similar to the charge transport, it is reasonable to expect that the asymmetric grain boundary would exhibit different property of thermal transport from that of the symmetric grain boundary.

In this paper, we adopt the nonequilibrium molecular dynamics (NEMD) method[21, 22, 23] to simulate the heat transport across the asymmetric grain boundary between armchair graphene and zigzag graphene. We show that the Kapitza conductance and the thermal conductivity have strong dependence on the temperature. Furthermore, surprising thermal rectification phenomenon has been observed in the graphene with such asymmetric grain boundary. Our results provide a practical choice for designing thermal rectifier in polycrystalline graphene without delicate atomic engineering.

Figure 1 shows the atomic structure of the asymmetric grain boundary connecting the armchair and the zigzag regions. This structure has been denoted as a boundary structure between the armchair graphene and the zigzag graphene[24] while the electronic transport across that has been studied [13, 25]. This structure is composed of a periodic array of 5-pentagon and 7-heptagon topological defects. According to the mismatch of the period of the zigzag part and the armchair part, this asymmetric grain boundary shows peculiar 7-5-7 structure while the standard pentagon-heptagon dislocation cores would flip their orientations from 5-7 to 7-5[24]. In spite of the lattice mismatch, the formation energy of this asymmetric grain boundary is much smaller than the typical energy of the bare edges in graphene[26].

In all simulations, velocity Verlet algorithm is used to integrate the equation of motions[27]. Periodic boundary condition is imposed on the direction parallel to the grain boundary. Along the direction perpendicular to the grain boundary, fixed boundary condition is applied on the green atoms in the Figure 1. The brown atoms in Figure 1 are coupled to *Nosé – Hoover* heat baths[28], whose

temperatures are set to  $T_{high}$  and  $T_{low}$ , respectively, to generate the temperature gradient. **The length of heat bath used in our simulation is around 1 nm. We have carefully tested the effect of the heat bath length on our results. The quantity of the calculated thermal rectification is only slightly affected by the length of heat bath.** A recent parameter-modified Tersoff potential is used to describe the atomic interaction[29], which has been verified to give the right velocities of the acoustic-phonon which is crucial in thermal transport. The new parametrized potential considerably improves the computational values of the lattice thermal conductivity and makes them in good agreement with the experimental results[18, 30]. After the system reaches to the steady state, the heat flux could be calculated by the energy flowing from the heat bath to the system[31]. The thermal conductivity could be obtained according to the Fourier's law

$$\kappa = \frac{Jd}{\Delta T_1 wh} \quad (1)$$

In the equation,  $J$  represents the heat flux,  $d$  is the length of sample,  $\Delta T_1$  is the temperature difference between  $T_{high}$  and  $T_{low}$ ,  $w$  and  $h$  is the width and height of the monolayer graphene, respectively. The temperature usually shows significant temperature jump at the grain boundary region, the boundary conductance is defined as:

$$G = \frac{J}{\Delta T_2} \quad (2)$$

$J$  is the heat flux and  $\Delta T_2$  is the temperature jump at the boundary[20].

Before starting the simulation, the atomic structure has been fully optimized in a microcanonical ensemble by conjugate gradient method for ensuring the forces on each atom being less than  $10^{-8}$  eV/Å. Applying the *Nosé – Hoover* thermostat on two ends about 1 ns, the system reaches steady equilibrium. The heat flux and the temperature gradient is obtained by the average of 4 ns. The time step of the simulation is set to 1 fs. The simulation time has been tested to be enough for convergence. The width of the period parrallel to the grain boundary is about 3 nm and the height of the sample is set to be the distance between graphite layers about 3.35 Å[20].

At first, we calculate the thermal conductivity of pure graphene to validate our simulation results. While the length of the sample is about 10 nm and 25 nm under the simulation temperature around 300 K, the thermal conductivity is about 327 W/(mK) and 455 W/(mK) respectively, which is in good agreement with the previous NEMD simulation results [32, 33, 34]. Under the same simulation condition, the thermal conductivity of the graphene sheet with the asymmetric grain boundary reduced to only around 240 W/(mK) which becomes considerably lower than the pure graphene. The apparent reduction of thermal conductivity is attributed to the strong phonon scattering at grain boundary.

Superior boundary thermal conductance has been observed in the simulation. At room temperature, the boundary thermal conductance of the asymmetric grain boundary is about  $1.5 \times 10^{10}$  W/m<sup>2</sup>K which is much larger than

the reported value of grain boundaries in nanocrystalline diamond thin films[35] and silicon-silicon (001)  $\Sigma 29$  grain boundaries[36, 37]. Our results is slightly lower than the previous reported boundary thermal conductance of the symmetric grain boundary[20]. The misorientation angle of this asymmetric grain boundary is 30 degree which is larger than that of the reported symmetric grain boundaries. The large misorientation angle would induce the increase of the defects densities and the probability of the phonon-boundary scattering, which would finally reduce the thermal boundary conductance.

The temperature dependence of the boundary thermal conductance and the thermal conductivity has been investigated systematically, which are shown in Figure 2(a) and 2(b), respectively. When the temperature increases up to 550 K, the thermal boundary conductance increases from  $1.3 \times 10^{10}$  W/m<sup>2</sup>K to  $2.0 \times 10^{10}$  W/m<sup>2</sup>K. The similar trend has also been observed in the Si-Ge interfaces[38] and the Kr-Ar interfaces[39]. While at the high temperature around 600K, the boundary thermal conductance suddenly drops. This could be attributed to the transformation of atomic structure of the grain boundary. The C-C bonds in the array of 5-pentagon and 7-heptagon topological defects broken has been observed which reveals the structural instability of the asymmetric grain boundary at high temperature. The thermal transport depending on the atomic structure of the grain boundary was also found in a previous study [20]. The thermal conductivity follows the same relation as the boundary thermal conductance respecting to the temperature, which has been reported in previous theoretical study on defect free graphene[17, 40], while the sudden drop of the thermal conductivity near 600 K could be also attributed to the atomic structural changing of the grain boundary.

The monotonic increase of thermal boundary conductance with the rising of temperature before the structure changing could be interpreted by considering the following two factors. Firstly, the thermal fluctuation increases with the rise in temperature. Consequently, the probability of inelastic phonon scattering increases at the grain boundaries[38]. The optical phonon with high frequency might break down into numerous acoustic phonons with low frequency. These acoustic phonons have higher probability of transmission comparing to high frequency optical phonon due to the limited width of the asymmetric grain boundary. Besides that, more acoustic phonon would be stimulated at high temperature which could also contribute to the increase of boundary thermal conductance.

It is interesting that we find the thermal conductivity and Kapitza conductance is asymmetric, i.e., the heat flux from armchair to zigzag is larger than that from zigzag to armchair, which suggests that such asymmetric grain boundary structure could be used to design a new kind of thermal rectifier.

The thermal rectification is found to be strongly temperature dependent and it could reach to as high as 74%. The thermal rectification versus the temperature difference  $|\Delta T|$  and the average temperature  $T$  are plotted in Figure 3(a) and 3(b). In Figure 3(a), the temperature difference between  $T_{high}$  and  $T_{low}$  has been set to 120 K and the simulation temperature varies from 200 K to 700 K. With the decrease of the simulation temperature, the thermal rectification

increases from 1.05 to 1.73. In Figure 3(b), the average simulation temperature  $\frac{T_{low}+T_{high}}{2}$  has been set to 400 K and the temperature difference between  $T_{high}$  and  $T_{low}$  varies from 40 K to 140 K. With the increasing of the temperature difference, the thermal rectification increase from 1.05 to 1.33. In both Figure 3(a) and 3(b), the thermal rectification increases with the rise in the temperature difference. The nanostructure like the carbon nanotube intramolecular junction[31], the asymmetric graphene ribbon[41], the carbon nanocone[42] and the hybrid graphene-graphane nanoribbon[43] has been proposed to be thermal rectifier in the past few years. The effect of thermal rectification in the asymmetric grain boundary revealed in this work is comparable to those in previous proposed systems.

**Furthermore, the thermal rectification is actually determined by the change of the phonon spectral overlap under opposite bias temperature[46]. In fact, the obvious difference between the phonon power spectrum of the armchair and zigzag graphene was verified in the previous theoretical studies [47, 48]. Besides that, the temperature-dependent phonon power spectrum, a typical characteristic of the nonlinear system, would change the phonon spectral overlap while the temperature bias is reversed, which results in the emerging of thermal rectification.** On the one hand, if the armchair part is under the high temperature, the power spectrum between these two parts is well matched and the thermal transport could be efficiently exchanged between two parts. On the other hand, if the armchair part is under the low temperature, the power spectrum of the armchair and the zigzag parts are shifted and the overlap is expected to be diminished. By the decrease of overlapping phonon spectrum, the efficiency of the thermal exchange between the armchair part and the zigzag part declines dramatically. While enlarging the temperature difference in two ends, the mismatch between the phonon spectrum of two parts would also increase therefore the thermal rectification is magnified. Under low temperature, the thermal conductivity of the graphene highly depends on the temperature[40], which indicates that the phonon spectrum shifted more considerably at low temperature than at high temperature by the same amount change of temperature. For this reason, with the same temperature difference, the overlap of phonon spectrum decreases more at low temperature than that at high temperature, therefore the effect of thermal rectification is amplified at low temperature. According to the phonon spectrum match/mismatch theory mentioned above, the results of our simulation could be well understood. **On the other hand, at the high temperature region more acoustic phonons would generate in the system. If more acoustic phonons are generated, the grain boundary with limited width would impose less impact on the thermal transport. In this case, the thermal rectification would also decrease at the high temperature region.**

In summary, we have found that the Kapitza conductance across the grain boundary and the thermal conductivity are strongly temperature-dependent. Surprisingly, the asymmetric heat flux across the asymmetric zigzag-armchair

grain boundary is observed. It provides a potential candidate for future design of carbon-based thermal rectifier which has attracted a lot of attention recently [47].

**Acknowledgement**

This work is supported by NSF of China, the Special Funds for Major State Basic Research, the Research Program of Shanghai municipality.

**References**

- [1] A. K. Geim and K. S. Novoselov, *Nat. Mater.* **6**, 183 (2007).
- [2] A. K. Geim, *Science* **324**, 1530 (2009).
- [3] T. J. Booth, P. Blake, R. R. Nair, D. Jiang, E. W. Hill, U. Bangert, A. Bleloch, M. Gass, K. S. Novoselov, M. I. Katsnelson, and A. K. Geim, *Nano Lett.* **8**, 2442 (2008).
- [4] C. Gomez-Navarro, R. T. Weitz, A. M. Bittner, M. Scolari, A. Mews, M. Burghard, and K. Kern, *Nano Letters* **7**, 3499 (2007).
- [5] A. A. Balandin, S. Ghosh, W. Z. Bao, I. Calizo, D. Teweldebrhan, F. Miao, and C. N. Lau, *Nano Letters* **8**, 902 (2008).
- [6] F. Wang, Y. B. Zhang, C. S. Tian, C. Girit, A. Zettl, M. Crommie, and Y. R. Shen, *Science* **320**, 206 (2008).
- [7] K. S. Kim, Y. Zhao, H. Jang, S. Y. Lee, J. M. Kim, J. H. Ahn, P. Kim, J. Y. Choi, and B. H. Hong, *Nature* **457**, 706 (2009).
- [8] A. Reina, X. T. Jia, J. Ho, D. Nezich, H. B. Son, V. Bulovic, M. S. Dresselhaus, and J. Kong, *Nano Lett.* **9**, 30 (2009).
- [9] X. S. Li, W. W. Cai, J. H. An, S. Kim, J. Nah, D. X. Yang, R. Piner, A. Velamakanni, I. Jung, E. Tutuc, S. K. Banerjee, L. Colombo, and R. S. Ruoff, *Science* **324**, 1312 (2009).
- [10] W. W. Cai, A. L. Moore, Y. W. Zhu, X. S. Li, S. S. Chen, L. Shi, and R. S. Ruoff, *Nano Lett.* **10**, 1645 (2010).
- [11] X. S. Li, C. W. Magnuson, A. Venugopal, J. H. An, J. W. Suk, B. Y. Han, M. Borysiak, W. W. Cai, A. Velamakanni, Y. W. Zhu, L. F. Fu, E. M. Vogel, E. Voelkl, L. Colombo, and R. S. Ruoff, *Nano Lett.* **10**, 4328 (2010).
- [12] R. Grantab, V. B. Shenoy, and R. S. Ruoff, *Science* **330**, 946 (2010).
- [13] O. V. Yazyev and S. G. Louie, *Nat. Mater.* **9**, 806 (2010).
- [14] D. Gunlycke and C. T. White, *Phys. Rev. Lett.* **106**, 136806 (2011).
- [15] J. Lahiri, Y. Lin, P. Bozkurt, Oleynik, II, and M. Batzill, *Nat. Nanotechnol.* **5**, 326 (2010).
- [16] L. Z. Kou, C. Tang, W. L. Guo, and C. F. Chen, *ACS Nano* **5**, 1012 (2011).
- [17] J. N. Hu, X. L. Ruan, and Y. P. Chen, *Nano Lett.* **9**, 2730 (2009).

- [18] J. Haskins, A. Kinaci, C. Sevik, H. Sevincli, G. Cuniberti, and T. Cagin, *ACS Nano* **5**, 3779 (2011).
- [19] J. N. Hu, S. Schifflì, A. Vallabhaneni, X. L. Ruan, and Y. P. Chen, *Appl. Phys. Lett.* **97**, 133107(2010).
- [20] Akbar Bagri, Sang-Pil Kim, Rodney S. Ruoff, and Vivek B. Shenoy, *Nano Lett.* **11**, 3917 (2011).
- [21] N. Yang, G. Zhang, and B. Li, *Nano Lett.* **65**, 144306 (2002)
- [22] Z. X. Guo, D. Zhang, and X. G. Gong, *Appl. Phys. Lett.* **95**, 163103 (2009).
- [23] Z. X. Guo, D. Zhang, Y. T. Zhai, and X. G. Gong, *Nanotechnology* **21**, 285706 (2010).
- [24] Yuanyue Liu and Boris I. Yakobson, *Nano Lett.* **10**, 2178 (2010).
- [25] Xiao-Fei Li, Ling-Ling Wang, Ke-Qiu Chen, and Yi Luo, *J. Chem. Phys. C* **115**, 12616 (2011).
- [26] P. Koskinen, S. Malola; H. Hakkinen, *Phys. Rev. Lett.* **101**, 115502 (2008).
- [27] Z. X. Guo and X. G. Gong, *Front. Phys. China* **4**, 389 (2009).
- [28] S. Nosé, *J. Chem. Phys.* **81**, 511 (1984) W. G. Hoover, *Phys. Rev. A* **31**, 1695 (1985).
- [29] L. Lindsay and D. A. Broido, *Phys. Rev. B* **81**, 205441 (2010).
- [30] L. Lindsay, D. A. Broido, and N. Mingo, *Phys. Rev. B* **82**, 161402 (2010).
- [31] G. Wu and B. W. Li, *Phys. Rev. B* **76**, 085424 (2007).
- [32] Z. Y. Ong and E. Pop, *Phys. Rev. B* **84**, 075471 (2011).
- [33] Qing-Xiang Pei, Zhen-Dong Sha, and Yong-Wei Zhang, *Carbon* **49**, 4752 (2011).
- [34] S. K. Chien, Y. T. Yang, and C. K. Chen, *Appl. Phys. Lett.* **98**, 033107 (2011).
- [35] M. A. Angadi, T. Watanabe, A. Bodapati, X. C. Xiao, O. Auciello, J. A. Carlisle, J. A. Eastman, P. Keblinski, P. K. Schelling, and S. R. Phillpot, *J. Appl. Phys.* **99**, 114301 (2006).
- [36] P. K. Schelling, S. R. Phillpot, and P. Keblinski, *J. Appl. Phys.* **95**, 6082 (2004).



- [37] A. Maiti, G. D. Mahan, and S. T. Pantelides, *Solid State Commun.* **102**, 517 (1997).
- [38] V. Samvedi and V. Tomar, *Nanotechnology* **20**, 365701 (2009).
- [39] Y. F. Chen, D. Y. Li, J. K. Yang, Y. H. Wu, J. R. Lukes, and A. Majumdar, *Physica B* **349**, 270 (2004).
- [40] W. R. Zhong, M. P. Zhang, B. Q. Ai, and D. Q. Zheng, *Appl. Phys. Lett.* **98**, 113107 (2011).
- [41] N. Yang, G. Zhang, and B. W. Li, *Appl. Phys. Lett.* **95**, 033107 (2009).
- [42] N. Yang, G. Zhang, and B. W. Li, *Appl. Phys. Lett.* **93**, 243111 (2008).
- [43] A. Rajabpour, S. M. V. Allaei, and F. Kowsary, *Appl. Phys. Lett.* **99**, 051917 (2011).
- [44] B. W. Li, L. Wang, and G. Casati, *Phys. Rev. Lett.* **93**, 184301 (2004).
- [45] T. Yamamoto, K. Watanabe, and K. Mii, *Phys. Rev. B* **70**, 245402 (2004).
- [46] M. Yamada, Y. Yamakita, and K. Ohno, *Phys. Rev. B* **77**, 054302 (2008).
- [47] N. A. Roberts and D. G. Walker, *Int. J. Therm. Sci.* **50**, 648 (2011).

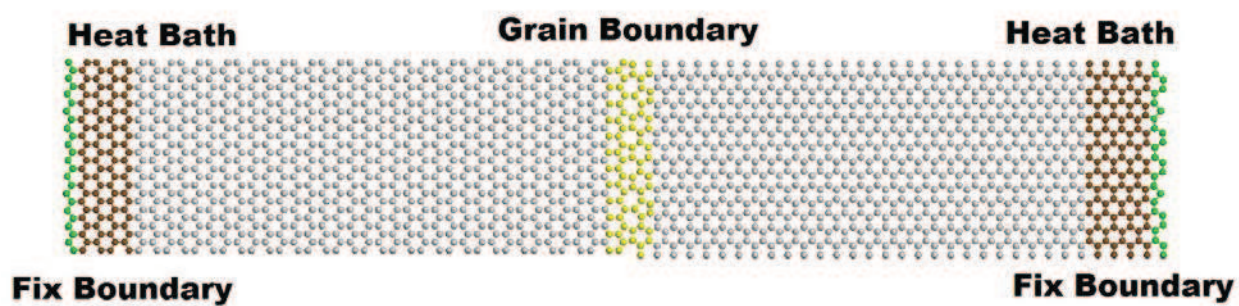


Figure 1: Structure of the asymmetric tilt grain boundary used in simulation. The green atoms are set to be applied fix boundaries. The brown atoms are set to be coupled to heat bath. The yellow atoms are the asymmetric boundary structure composed of 5-pentagon and 7-heptagon topological defects. The size of the sample is defined by the length between two heat bath.

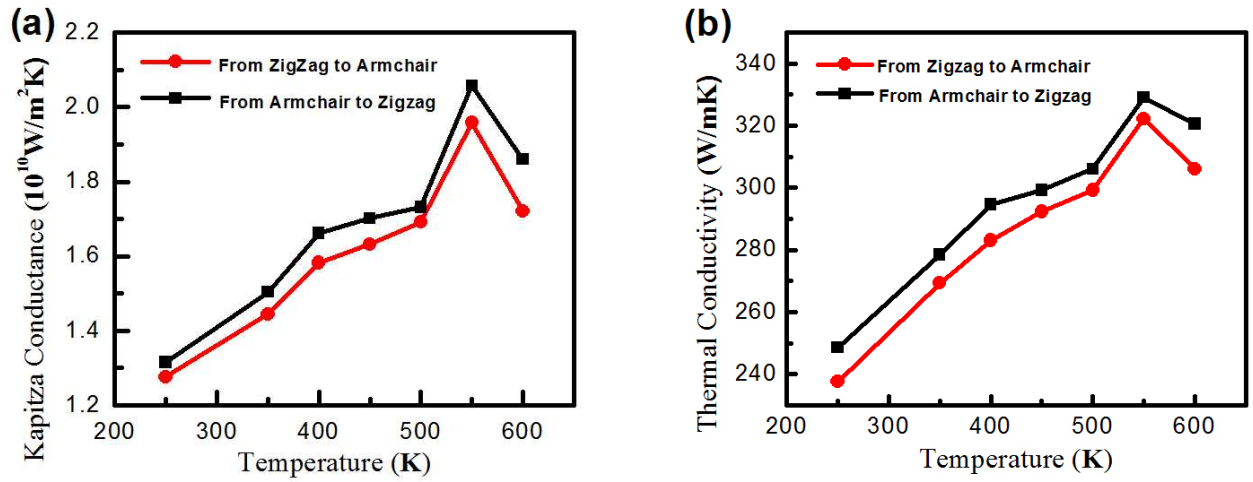


Figure 2: The temperature dependence of (a) the Kapitza conductance and (b) the thermal conductivity of armchair-zigzag asymmetric grain boundary. Both the Kapitza conductance and the thermal conductivity increase with the temperature increasing. The sudden drop of the Kapitza conductance and the thermal conductivity is attributed to the changing of the boundary structure at high temperature. In all the simulations, the size of the sample is 10 nm.

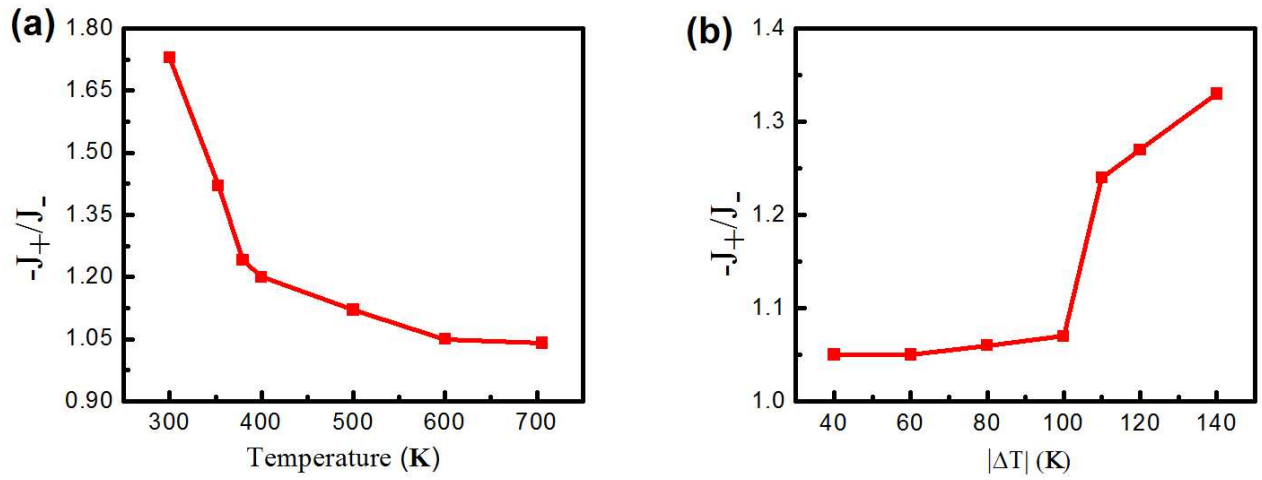


Figure 3: The thermal rectification versus (a) different temperature and (b) different temperature difference. In Figure 3(a) the temperature difference is set to be 120 K. In Figure 3(b) the simulation temperature is set to be 400 K. The effect of thermal rectification has been evaluated by the ratio of the asymmetric heat flux along two reverse directions.  $J_+$  means the heat flux from the armchair part to the zigzag part while  $J_-$  means that the heat flux from the zigzag part to the armchair part. In all the simulations, the size of the sample is 10 nm.